

Electronic Supplementary Information (ESI) for CrystEngComm

Jonna Jokiniemi*, Sirpa Peräniemi, Jouko. J. Vepsäläinen and Markku
Ahlgrén

Department of Chemistry, University of Joensuu, P.O. Box 111, 80101, Joensuu,
Finland

List of figures (Supplementary data)

Figure S1: ^{31}P -CP/MAS NMR spectrum of $[\text{Mg}(\text{CH}_3\text{PO}_3\text{CCl}_2\text{PO}_2\text{NC}_4\text{H}_8\text{O})(\text{H}_2\text{O})_3]_n$ (**1**)

Figure S2: ^{31}P -CP/MAS NMR spectrum of $[\text{Ba}(\text{CH}_3\text{PO}_3\text{CCl}_2\text{PO}_2\text{NC}_4\text{H}_8\text{O})(\text{H}_2\text{O})_2]_n$ (**2**)

Figure S3: ^{31}P -CP/MAS NMR spectrum of $[\text{Sr}_2(\text{CH}_3\text{PO}_3\text{CCl}_2\text{PO}_2\text{NC}_4\text{H}_8)_2(\text{H}_2\text{O})_{3.5}]_n$ (**3**)

Figure S4: FT-IR spectrum of $[\text{Mg}(\text{CH}_3\text{PO}_3\text{CCl}_2\text{PO}_2\text{NC}_4\text{H}_8\text{O})(\text{H}_2\text{O})_3]_n$ (**1**) in KBr pellet

Figure S5: FT-IR spectrum of $[\text{Ba}(\text{CH}_3\text{PO}_3\text{CCl}_2\text{PO}_2\text{NC}_4\text{H}_8\text{O})(\text{H}_2\text{O})_2]_n$ (**2**) in KBr pellet

Figure S6: FT-IR spectrum of $[\text{Sr}_2(\text{CH}_3\text{PO}_3\text{CCl}_2\text{PO}_2\text{NC}_4\text{H}_8)_2(\text{H}_2\text{O})_{3.5}]_n$ (**3**) in KBr pellet

Figure S7: A thermogravimetric curve of the starting material $(\text{C}_4\text{H}_8\text{ONH}_2)_2\text{CH}_3\text{PO}_3\text{C}-\text{Cl}_2\text{PO}_2\text{NC}_4\text{H}_8\text{O}$ performed in nitrogen atmosphere in a temperature range of 25–600 °C and at a heating rate of 5 °C /min.

Figure S8: A thermogravimetric curve of the starting material $(\text{C}_4\text{H}_8\text{NH}_2)_2\text{CH}_3\text{PO}_3\text{C}-\text{Cl}_2\text{PO}_2\text{NC}_4\text{H}_8$ performed in nitrogen atmosphere in a temperature range of 25–600 °C and at a heating rate of 5 °C /min.

Figure S9: A thermogravimetric curve of $[\text{Mg}(\text{CH}_3\text{PO}_3\text{CCl}_2\text{PO}_2\text{NC}_4\text{H}_8\text{O})(\text{H}_2\text{O})_3]_n$ (**1**) performed under synthetic air in a temperature range of 25–700 °C and at a heating rate of 5 °C /min.

Figure S10: A thermogravimetric curve of $[\text{Ba}(\text{CH}_3\text{PO}_3\text{CCl}_2\text{PO}_2\text{NC}_4\text{H}_8\text{O})(\text{H}_2\text{O})_2]_n$ (**2**) performed under synthetic air in a temperature range of 25–900 °C and at a heating rate of 5 °C /min.

Figure S11: A thermogravimetric curve of $[\text{Sr}_2(\text{CH}_3\text{PO}_3\text{CCl}_2\text{PO}_2\text{NC}_4\text{H}_8)_2(\text{H}_2\text{O})_{3.5}]_n$ (**3**) performed under synthetic air in a temperature range of 25–900 °C and at a heating rate of 5 °C /min.

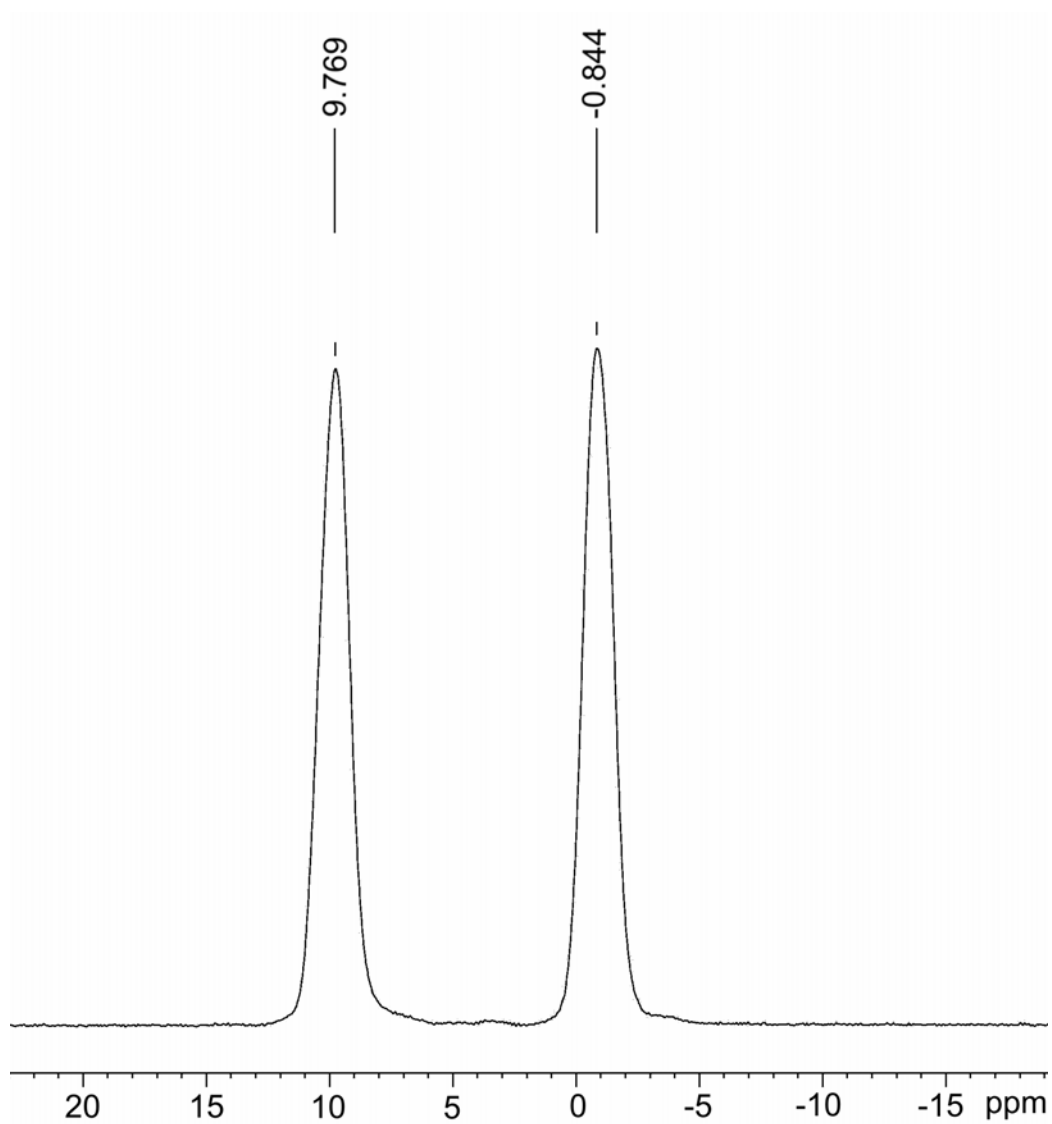


Figure S1: ^{31}P -CP/MAS NMR spectrum of $[\text{Mg}(\text{CH}_3\text{PO}_3\text{CCl}_2\text{PO}_2\text{NC}_4\text{H}_8\text{O})(\text{H}_2\text{O})_3]_n$ (**1**).

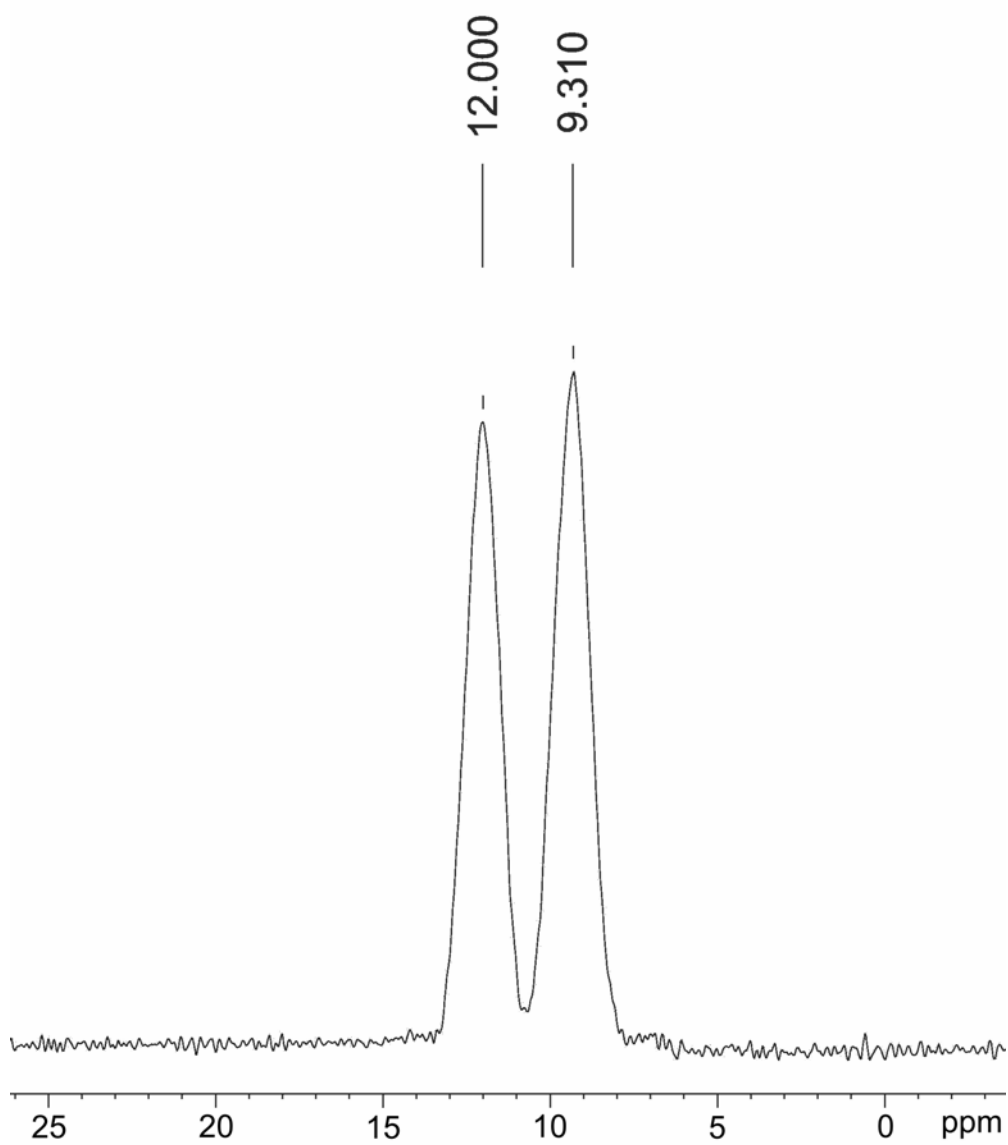


Figure S2: ^{31}P -CP/MAS NMR spectrum of $[\text{Ba}(\text{CH}_3\text{PO}_3\text{CCl}_2\text{PO}_2\text{NC}_4\text{H}_8\text{O})(\text{H}_2\text{O})_2]_n$ (**2**).

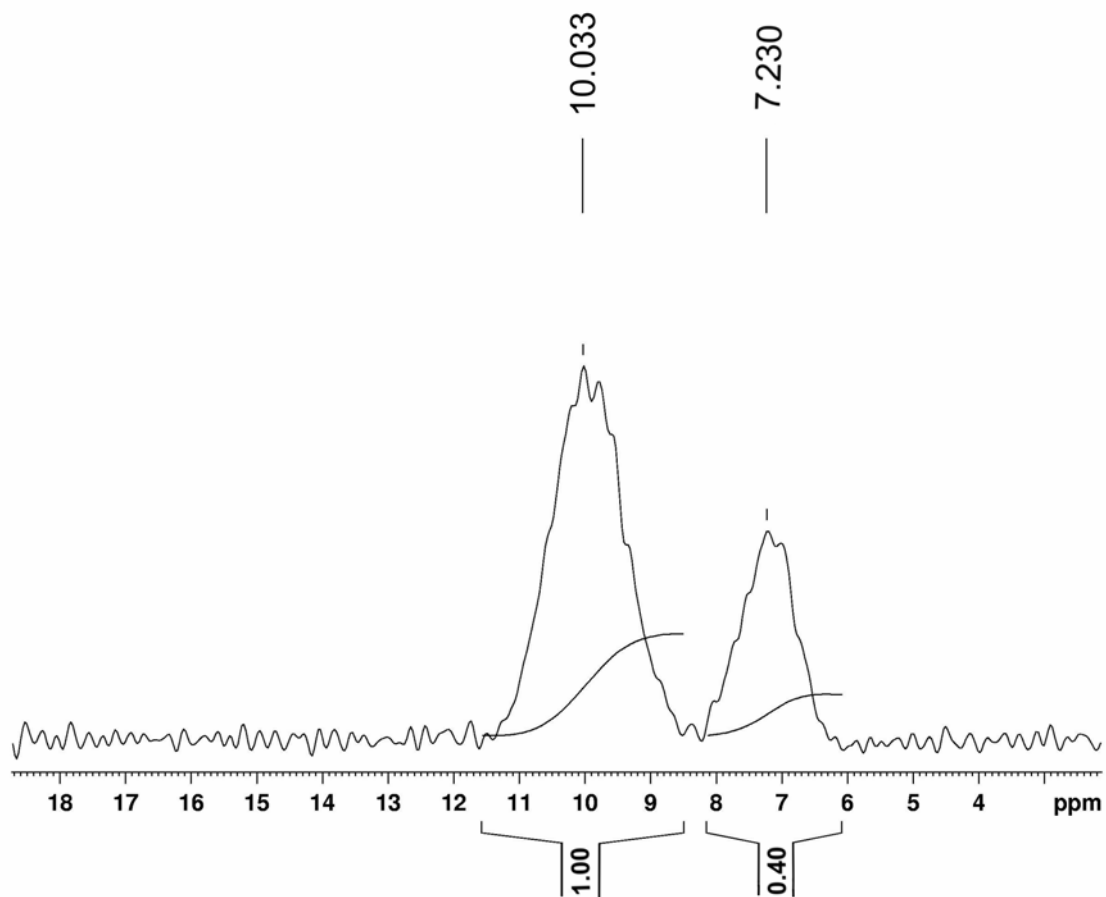


Figure S3: ^{31}P -CP/MAS NMR spectrum of $[\text{Sr}_2(\text{CH}_3\text{PO}_3\text{CCl}_2\text{PO}_2\text{NC}_4\text{H}_8)_2(\text{H}_2\text{O})_{3.5}]_n$ (**3**).

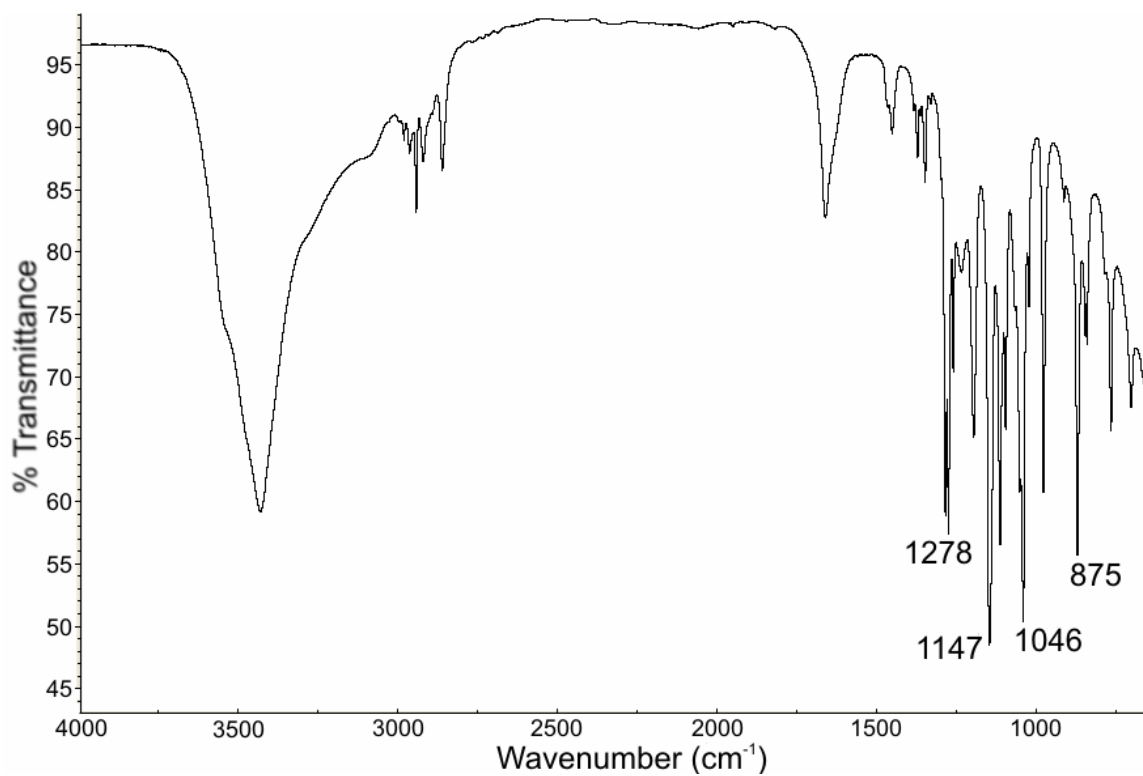


Figure S4: FT-IR spectrum of $[\text{Mg}(\text{CH}_3\text{PO}_3\text{CCl}_2\text{PO}_2\text{NC}_4\text{H}_8\text{O})(\text{H}_2\text{O})_3]_n$ (**1**) in KBr pellet.

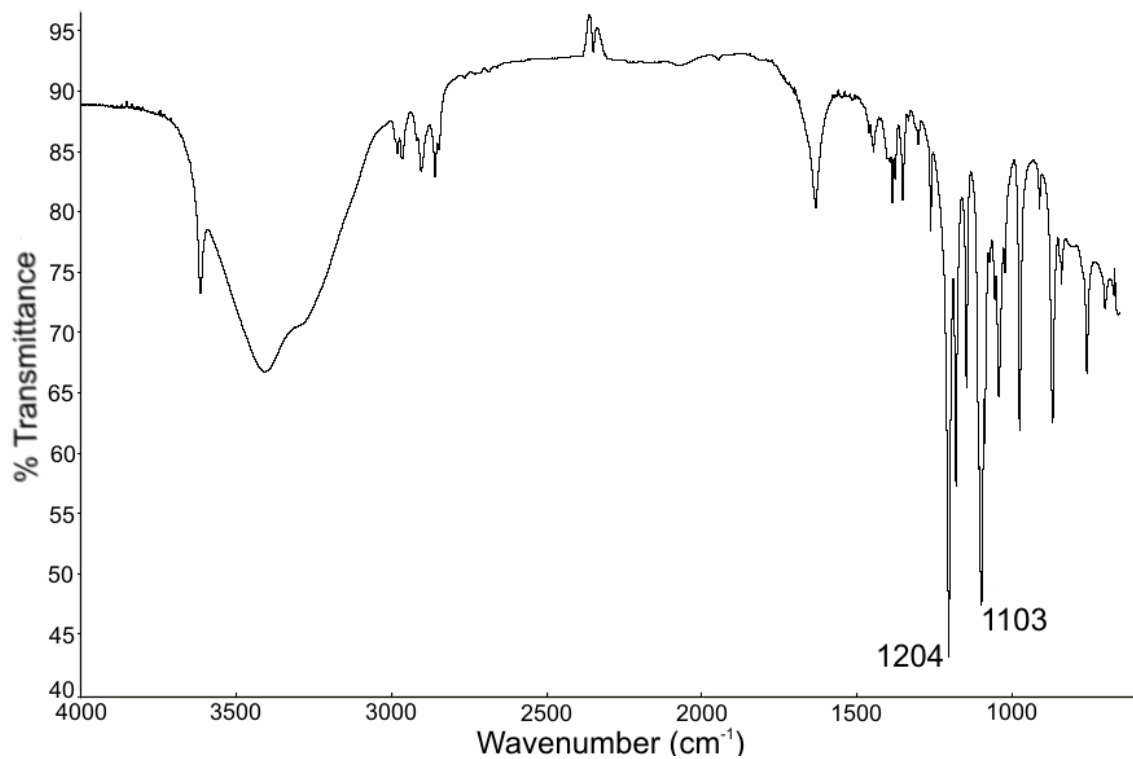


Figure S5: FT-IR spectrum of $[\text{Ba}(\text{CH}_3\text{PO}_3\text{CCl}_2\text{PO}_2\text{NC}_4\text{H}_8\text{O})(\text{H}_2\text{O})_2]_n$ (**2**) in KBr pellet.

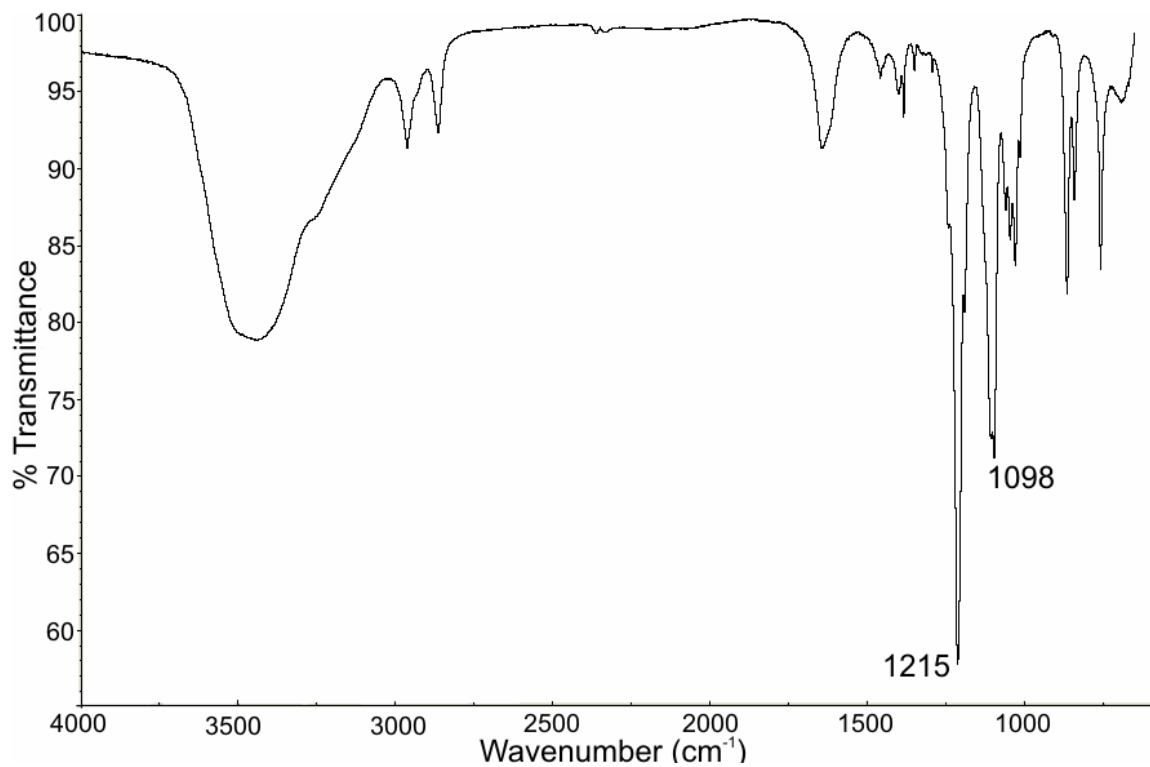


Figure S6: FT-IR spectrum of $[\text{Sr}_2(\text{CH}_3\text{PO}_3\text{CCl}_2\text{PO}_2\text{NC}_4\text{H}_8)_2(\text{H}_2\text{O})_{3.5}]_n$ (**3**) in KBr pellet.

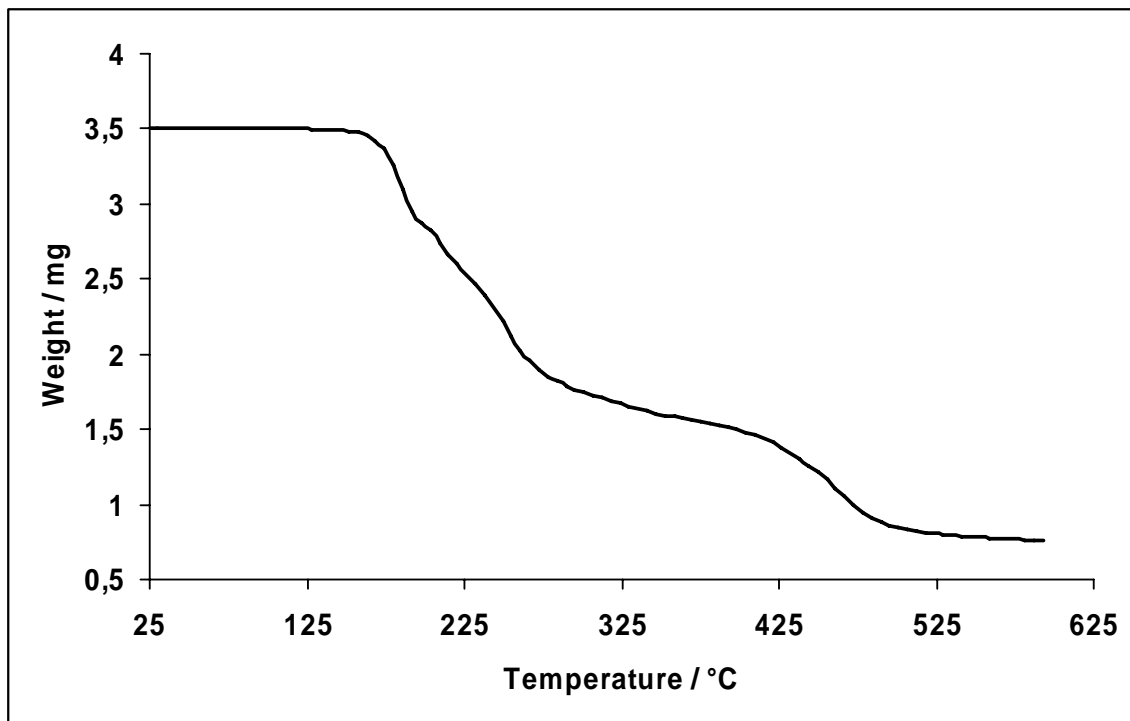


Figure S7: A thermogravimetric curve of the starting material $(\text{C}_4\text{H}_8\text{ONH}_2)_2\text{CH}_3\text{PO}_3\text{C}-\text{Cl}_2\text{PO}_2\text{NC}_4\text{H}_8\text{O}$ performed in nitrogen atmosphere in a temperature range of 25–600 °C and at a heating rate of 5 °C /min.

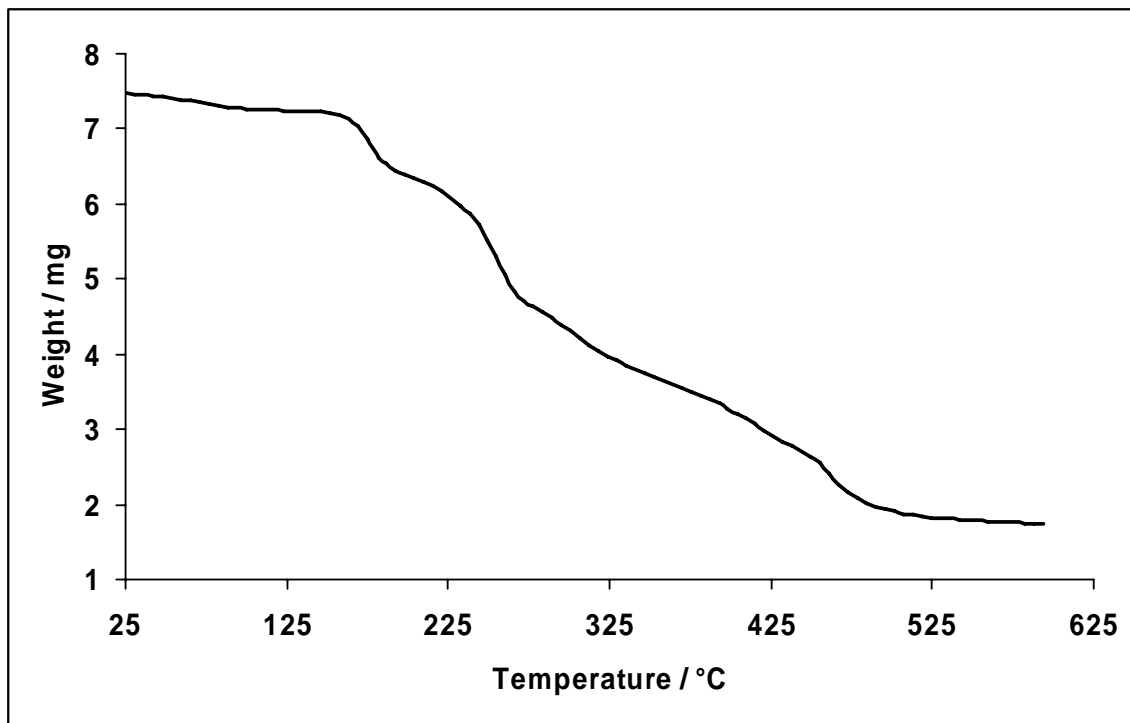


Figure S8: A thermogravimetric curve of the starting material $(C_4H_8NH_2)_2CH_3PO_3C-Cl_2PO_2NC_4H_8$ performed in nitrogen atmosphere in a temperature range of 25–600 °C and at a heating rate of 5 °C /min.

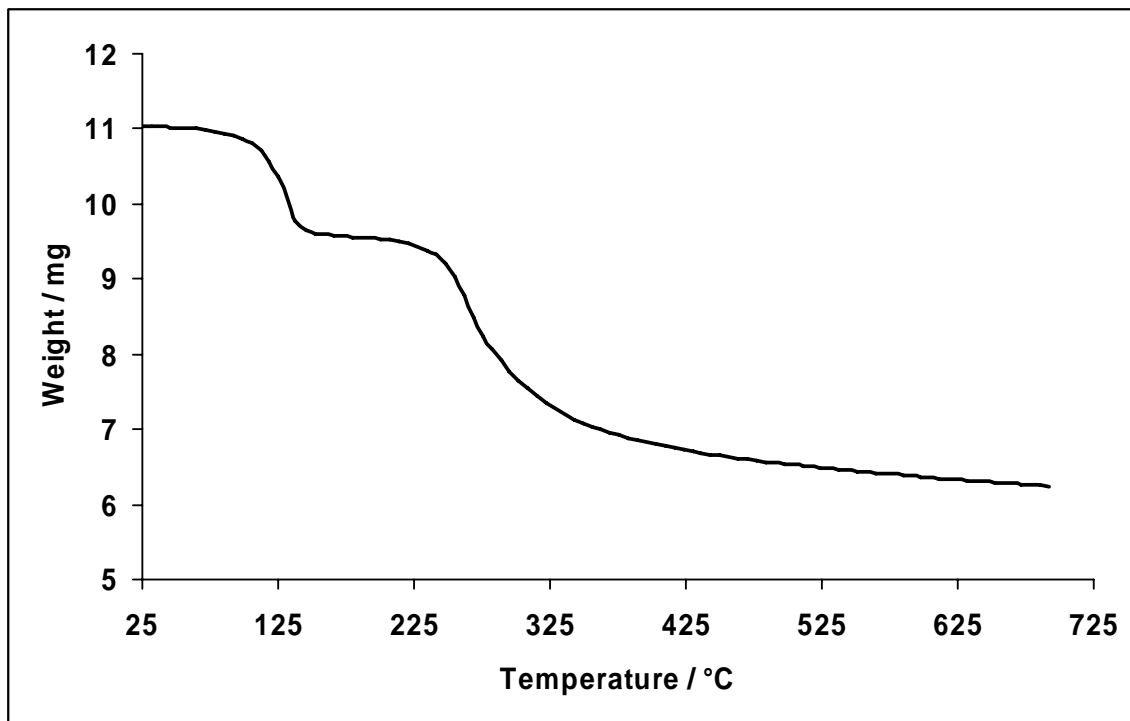


Figure S9: A thermogravimetric curve of $[\text{Mg}(\text{CH}_3\text{PO}_3\text{CCl}_2\text{PO}_2\text{NC}_4\text{H}_8\text{O})(\text{H}_2\text{O})_3]_n$ (**1**) performed under synthetic air in a temperature range of 25–700 °C and at a heating rate of 5 °C /min.

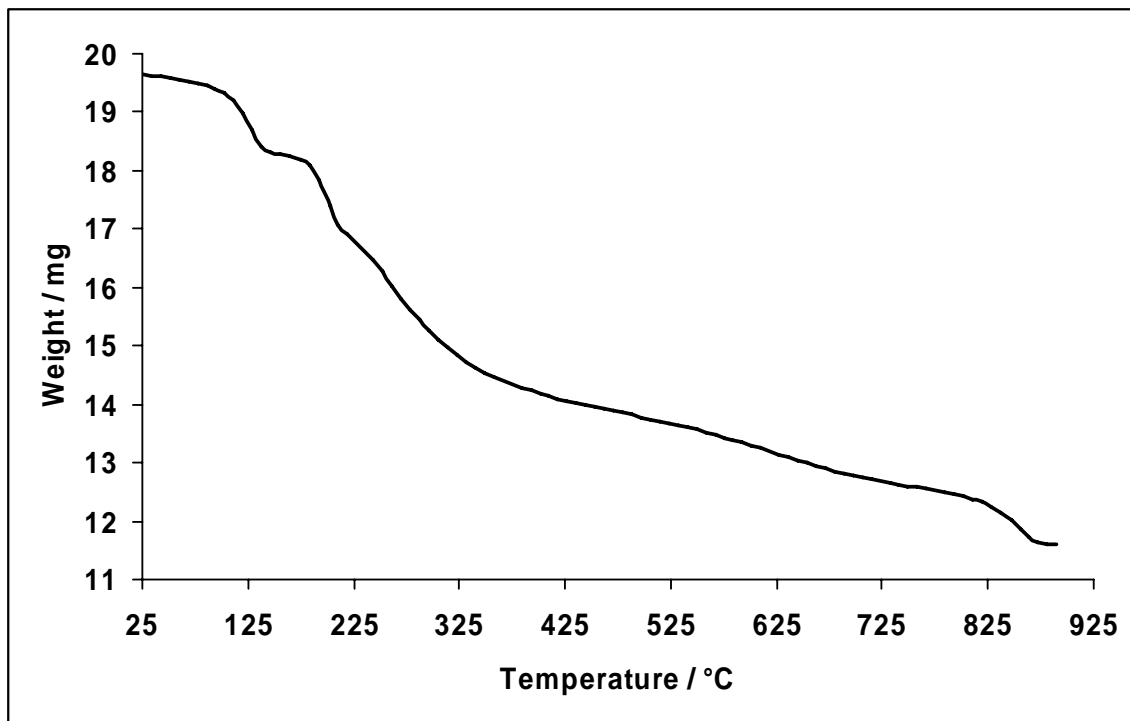


Figure S10: A thermogravimetric curve of $[\text{Ba}(\text{CH}_3\text{PO}_3\text{CCl}_2\text{PO}_2\text{NC}_4\text{H}_8\text{O})(\text{H}_2\text{O})_2]_n$ (**2**) performed under synthetic air in a temperature range of 25–900 °C and at a heating rate of 5 °C /min.

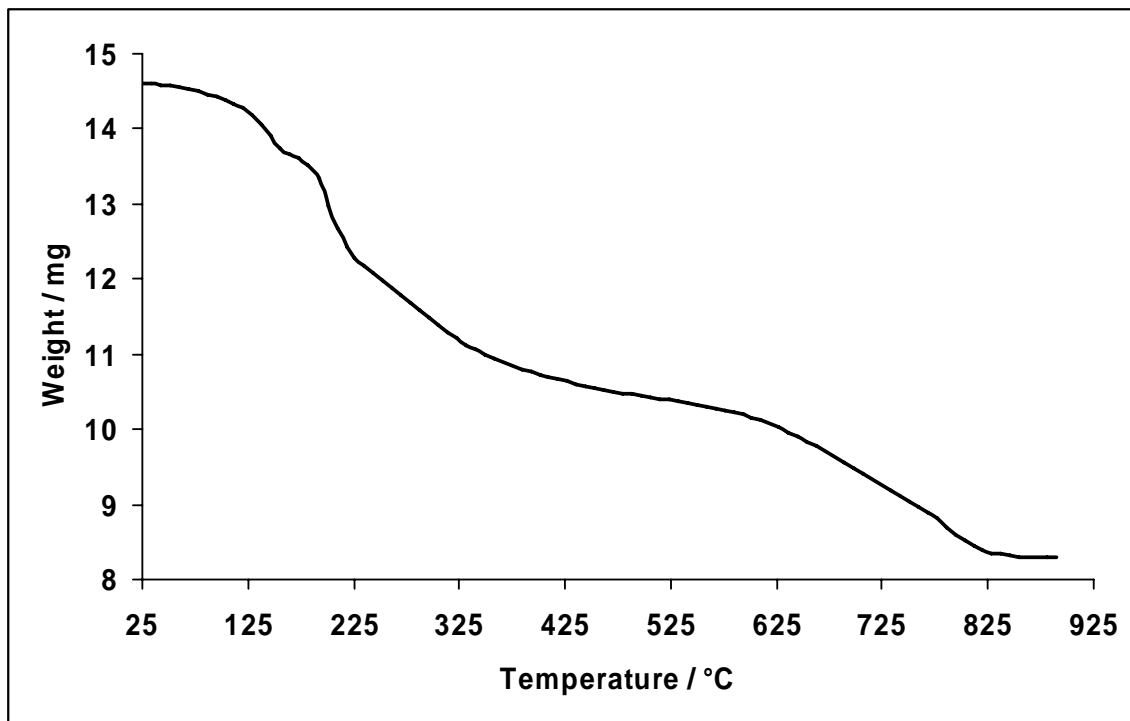


Figure S11: A thermogravimetric curve of $[\text{Sr}_2(\text{CH}_3\text{PO}_3\text{CCl}_2\text{PO}_2\text{NC}_4\text{H}_8)_2(\text{H}_2\text{O})_{3.5}]_n$ (**3**) performed under synthetic air in a temperature range of 25–900 °C and at a heating rate of 5 °C /min.